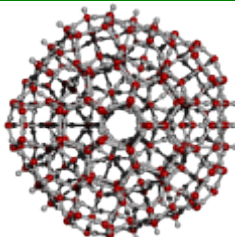


Evidence for Icosahedral Clusters

- ▼ [The radial distribution function](#)
- ▼ [Other support from diffraction data](#)
- ▼ [Support from clathrate structures](#)
- ▼ [Evidence from amorphous ice and low density water](#)



▼ [Other evidence](#)

The radial distribution function

Although the [icosahedral cluster model](#) can explain the anomalous properties of water, so can other models to varying extents. The strongest direct evidence for [this model](#) is the agreement with the radial distribution functions. The [CS](#) model was used to generate a radial distribution of the O···O distances. [Figure 1](#) compares this radial distribution function with that from the X-ray data at 4 °C [[9](#)], which shows a great deal of [fine structure](#). Although the peaks are in the same positions, they are less distinct in the X-ray data indicating the relative movements [expected of a liquid](#). There are 14 peaks or troughs in the $g_{OO}(r)$ plot, plus a further 36 inflections evident using the first derivative (that is, peaks and troughs in the $\Delta g_{OO}/\Delta r$ plot). All 50 positions show correspondence between the X-ray data and the calculated function for [CS](#), except that between about 7.9 Å and 8.5 Å where two peaks and troughs in the first derivative X-ray data only had corresponding inflections in the first derivative [CS](#) model data. If all 50 data are considered, the standard deviation of the differences between the X-ray data and the [CS](#) model data is less than 1% (0.065 Å). This correspondence is qualitatively indicative of the presence of the described clusters (or significantly large fractions of the clusters or partial clusters), and in agreement with more recent wide-angle X-ray diffraction measurements [[1755](#)] that are explained as a tetrahedral minority structuring within a more disorganized majority water structuring. There is also good correspondence with the O···O radial distribution functions derived from the neutron diffraction data, although this experimental data shows less fine structure [[36](#)].

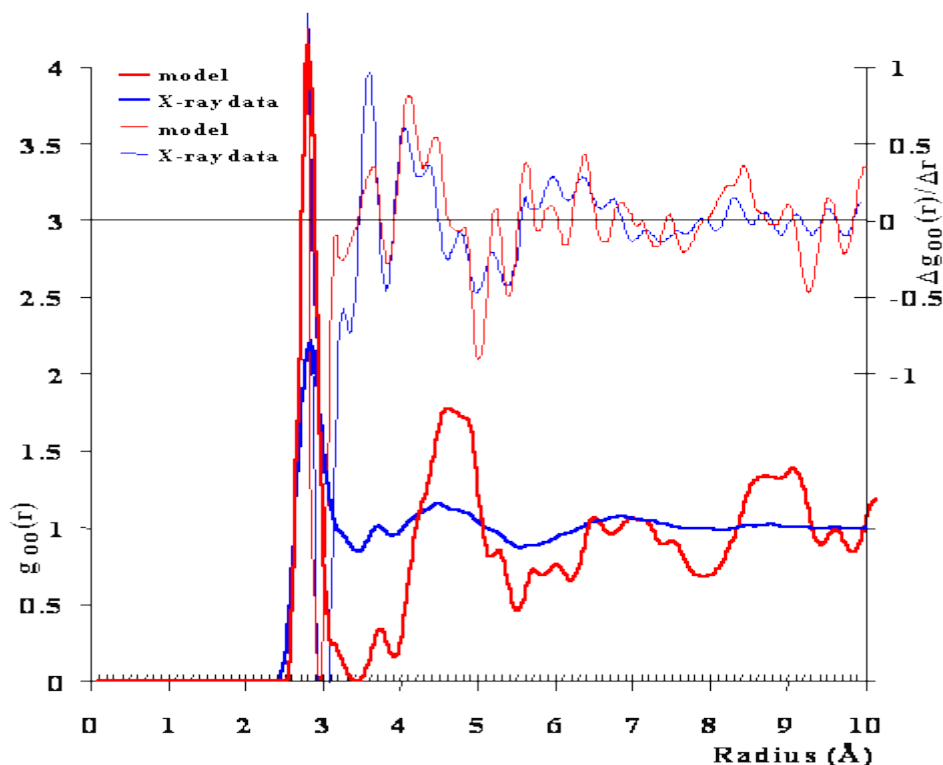


Figure 1. Comparison of the calculated oxygen radial distribution function from the model with the early, but information-rich, X-ray diffraction data of Narten [[9](#)] of near-surface water at 4 °C. There are 14 peaks or troughs plus a further 36 inflections evident using the first derivative (above, diffraction data scaled x 5).[Ⓔ]

| Key points in the RDF | | | |
|-----------------------|-------|----------------|-------|
| Peak/trough, Å | | Inflections, Å | |
| Model | X-ray | Model | X-ray |
| | | | |

| | | | | | |
|------|------|------|------|------|------|
| | | 2.69 | 6.36 | 2.65 | 6.35 |
| 2.81 | 2.83 | 2.90 | 6.65 | 2.99 | 6.59 |
| 3.44 | 3.46 | 3.16 | 6.86 | 3.25 | 6.75 |
| 3.73 | 3.72 | 3.26 | 7.06 | 3.34 | 6.99 |
| 3.91 | 3.91 | 3.63 | 7.12 | 3.60 | 7.15 |
| 4.52 | 4.49 | 3.81 | 7.30 | 3.80 | 7.35 |
| 5.52 | 5.55 | 4.09 | 7.47 | 4.05 | 7.56 |
| 7.00 | 6.86 | 4.28 | 7.64 | 4.24 | 7.65 |
| 7.90 | 7.83 | 4.46 | 7.91 | 4.36 | 7.89 |
| 8.72 | 8.79 | 4.73 | 8.00 | 4.60 | 8.07 |
| 8.88 | 8.79 | 4.82 | 8.44 | 4.76 | 8.31 |
| 9.08 | 9.03 | 5.01 | 8.59 | 4.99 | 8.52 |
| 9.43 | 9.18 | 5.24 | 8.65 | 5.19 | 8.70 |
| 9.63 | 9.42 | 5.39 | 8.83 | 5.36 | 8.90 |
| 9.85 | 9.62 | 5.61 | 9.00 | 5.60 | 9.10 |
| | 9.84 | 5.76 | 9.27 | 5.71 | 9.30 |
| | | 5.95 | 9.52 | 5.95 | 9.51 |
| | | 6.11 | 9.72 | 6.15 | 9.72 |

Recent X-ray diffraction data has confirmed the peak at about 3.4 Å and the double-peak feature at about 4.5 Å [1631,1788a/c]. Also other X-ray diffraction data on supercooled water has reinforced the above observations and supports the presence of clathrate-like structures in water and their increase at low (supercooled) temperatures [1476].^d

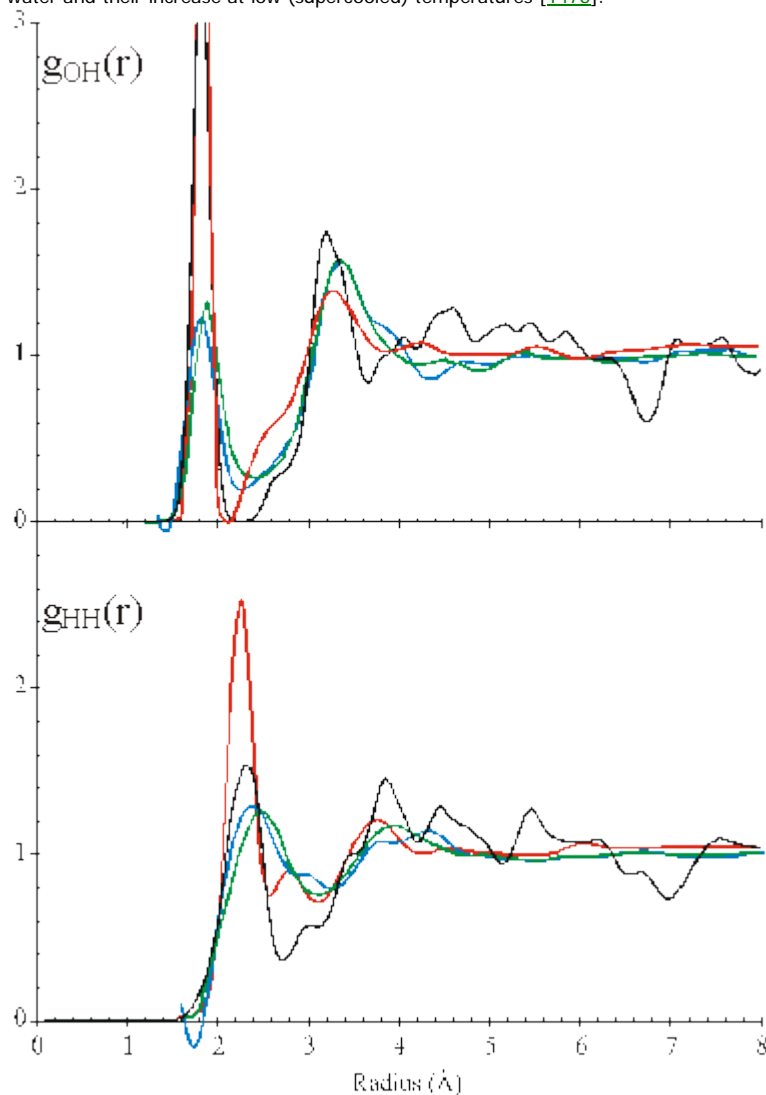


Figure 2. Comparison of the calculated O...H and H...H radial distribution functions of CS (black) with the published neutron diffraction data of water; red [35], blue [17], green[37].^e

The 2.8 Å peak from CS shows the presence of 4.34 nearest neighbors where 0.34 of these are contributed by the shoulder evident at about 3.2 Å. This compares well with the reported 4.4 nearest neighbors as calculated from the diffraction data [8], which also includes the shoulder at 3.2 Å as does an *ab initio* quantum mechanical/molecular mechanics molecular dynamics simulation study [922]. The size of the 3.7 Å peak compared to the 2.8 Å peak (0.69:4) from CS is close to that required from the radial distribution function (Fig. 1). It is also

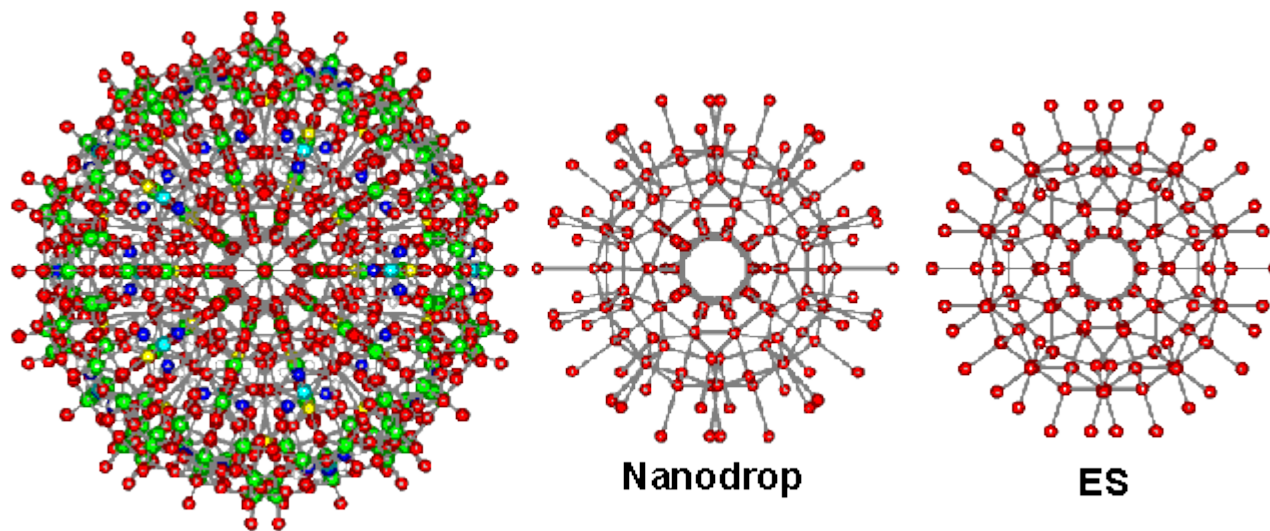
possible that very weakly hydrogen-bonded molecules may occupy a small number of the [interstitial sites](#) as found in effectively-powdered hexagonal ice [154]. If only 1% of the water molecules occupied such sites, which is well within the 5% limit [13] possible, this peak would increase by about 50% due to multiple interactions. The presence of cyclic pentagons increases the number of second-neighbor distances, at between 4 - 5 Å, to first-neighbor distances in the ratio of 13.4:4 in contrast to the 12:4 ratio in [ice Ih](#) or [ice Ic](#) based structures and the substantially lower ratio in two-state structures containing [ice-two](#) [22]. However, it is quite difficult quantifying such ratios as they are entirely dependent on the cut-off distances used. ▲

The radial distribution functions of O...H and H...H distances can be calculated from the model (Fig.2). This is less useful for testing the model, however, due to the lack of detail in the neutron scattering data, its variability between laboratories, the higher temperatures used (25 °C), the presence of D₂O and the necessary, but possibly misleading, assumptions that must be made when calculating from the model that the hydrogen bonds are linear and all hydrogen-bonding arrangements are equally probable. However the model gives H...H peaks at 2.35 Å, 3.9 Å and 4.6 Å with a small peak at 2.9 Å and O...H peaks at 1.85 Å and 3.3 Å with smaller peaks at 4.55 Å and 5.25 Å similar to published data [17, 35, 37].

There is no doubt that all the diffraction data is compatible with the presence of significantly large amounts of tetrahedrally hydrogen bonded water molecules in liquid water as described in [hydrogen bonding](#) and [cluster equilibria](#).

Other support from diffraction data

Support for the structure of [ES](#) comes from its agreement with radial distribution functions of solutions, supercooled water, [LDA](#) and water nanodroplets. Liquid water contains a considerable amount of order that extends almost a nanometer at ambient temperatures [1866]. The cavity-cavity distribution function of supercooled water peaks at 5.5 Å [38] and the neon-neon distribution function in water peaks at 6 Å [38]. Both values are close to the cavity-cavity distribution function peak of [ES](#) at 5.4 Å. The radial distribution function of [ES](#) around its center consists of a number of [spherical shells](#) surrounding a dodecahedral cavity, where structure-forming ions or solutes may reside. The radius of this dodecahedron is 3.94 Å, agreeing with the minimum cage radius found [39], at 3.9 Å, and the average Kr...O distance found in cold (4 ± 5 °C) aqueous krypton solutions under 110 bar pressure [157]. This last study [157] also gave the Kr...O second shell distance of 6.6 Å in exact [agreement](#) with the [ES](#) model. The inner four shells of [ES](#), consisting of 160 water molecules (20 H₂O at 0.39 nm; 20 H₂O at 0.66 nm; 60 H₂O at 0.79 nm; 60 H₂O at 1.06 nm, see below right), have been found in almost identical positions and orientations within a cavity-encapsulated icosahedral nanodrop of water (see center below) in a polyoxomolybdate (see left below, 20 H₂O @ 0.38-0.40 nm; 20 H₂O at 0.65-0.68 nm; 60 H₂O at 0.76-0.79 nm; 60 O atoms (mostly H₂O) in hydrated molybdate at 1.06-1.07 nm) [417]. More details of this hydration are [shown elsewhere](#).

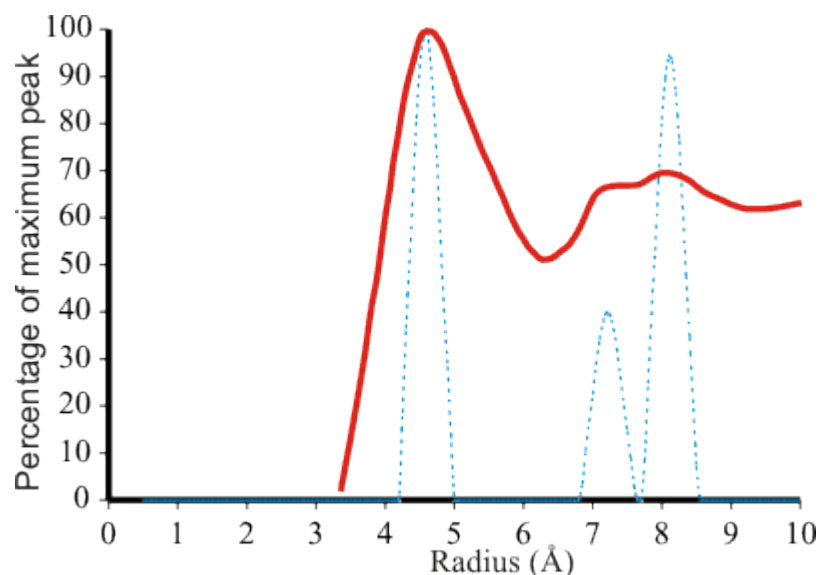


An cluster of silicon atoms (*i.e.* Si₂₈₀) with identical icosahedral structuring to [ES](#) has [been predicted](#) [990a], and found by molecular dynamics [990b], as a stable clustering in nanosized droplets of liquid silicon with a 15% reduced melting point over normal crystalline silicon.

Small-angle X-ray scattering (SAXS) has confirmed the presence of density fluctuations in liquid water on a physical length-scale of ~1.4 nm due to fluctuations between tetrahedral-like ([ES-like](#)) and hydrogen-bond distorted ([CS-like](#)) structures [1604].

Support from clathrate structures

There are many examples of the formation of dodecahedral clathrates in aqueous solutions [26, 27]. Dodecahedral clathrates can form with small molecules including the noble gases (except He which is too small), NH₄⁺, H₃O⁺, Cs⁺, N₂, O₂, CH₄ [349], H₂S, CO₂, (H₂)₂ and (H₂)₄, C₂H₆ and C₃H₈. Where formed, the stability of the (poorly formed) crystals depends on the pressure (generally greater than 1 MPa). Clathrate clusters have also been proposed as a contributing reason to why anesthetics like chloroform and nitrous oxide have their action [733]. Dodecahedral clusters containing NH₄⁺, K⁺ and Cs⁺ have also been found in ionized liquid water in the gas phase by mass spectrometry [26; see also [magic number ions](#)]. Such cavity formation is easy in water, increasing the strength of hydrogen-bonding in their neighborhood [31]. The [Hofmeister](#) series, whereby ions affect the stability of proteins in solution by either creating or destroying the structure of water, may be explained in part by how well large ions may sit passively in the dodecahedra, stabilizing [ES](#), relative to how strongly they create their own environment [40]. Cations that stabilize proteins in solution also create low-density water [29]. Theoretical studies have shown that the full icosahedral cluster (H₂O)₂₈₀ and, to a lesser but still significant extent, its central (H₂O)₁₀₀ core both stabilize the central dodecahedral cluster (H₂O)₂₀ and help stabilize the formation of clusters with contained molecules (*i.e.* clathrates) [1619].



The tetramethylammonium ion (TMA) is most effective [29] at stabilizing proteins and its effect on the structure of water has been investigated. In ES (dotted blue, right), expansion of the inner cavity to a radius of 4.60 Å, due to charge or steric effects, causes the next two shells in ES to expand to 7.23 Å (smaller peak) and 8.13 Å (larger peak). These three peaks may be related to those found at 4.6 Å, 7.2 Å (smaller peak) and 8.2 Å (larger peak) around the tetramethylammonium ion of 0.5 M TMA⁺Cl⁻ in D₂O (solid red, right) [39], as the 4.6 Å radius for the dodecahedral cavity is identical to half the sum of the TMA ion (6.34 Å) [545] and water molecule (2.85 Å) diameters. TMA solutions increase the solubility ('salt-in') small hydrophobes [1789] in agreement with the expectation from the ES model.

The ES structure provides about 1.4 dodecahedral sites per molecule for a 0.5-M solution. When higher concentrations of TMA⁺Cl⁻ were used, demanding more dodecahedral sites than can be provided by ES, the neutron diffraction peak detail was lost. In solutions of TMA⁺Cl⁻, the chloride had a co-ordination number to water of five and the TMA⁺...Cl⁻ distance was 5.3 Å [39]. Both agree with the chloride ion sitting asymmetrically in a nearby pentagonal box to a TMA ion situated within a dodecahedron, as this gives a co-ordination number of five to a dodecahedral face and a TMA⁺...Cl⁻ distance of 5.34 Å, given a (reasonable) H₂O...Cl⁻ distance of 3.24 Å. This study [39] also showed little effect of the salt on the structure of water despite the presence of water dodecahedra, which strengthens the argument that such dodecahedral structures are present in pure water. Analysis of the hydrogen bond angles indicates an increased degree of orientational ordering comparable to that occurring in water over 20 °C colder [211]. At high salt concentrations where more than one dodecahedral site is required per 70 water molecules, further sites may arise from tessellated, if distorted, dodecahedra (five water molecules per dodecahedron site, 6.1 Å between interstitial sites) or a tessellated structure formed from dodecahedra separated by single pentagonal boxes (25 water molecules per dodecahedron site, as may be present in aqueous dimethyl sulfoxide solutions [342], 10.6 Å between large interstitial sites and 5.3 Å between large and small interstitial sites). This latter structuring may also be indicated at the phase transitions noticed in concentrated salt solutions (~2M) [556], due to the ions breaking through their solvent-separated hydrated structures. Microwave dielectric relaxation measurements have indicated a critical behavior of water at a mole fraction (x_w) of 0.83 [6]. This can be explained by tessellated water dodecahedra, which have the required number of interstitial sites per water molecule ($x_w = 0.83$).

Evidence from amorphous ice and low density water

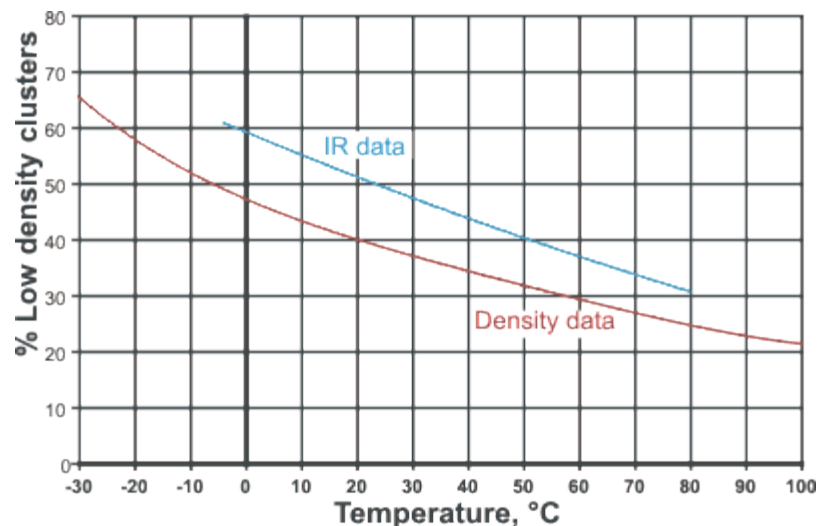
LDA is expected to be thermodynamically continuous with liquid water [16] and it certainly gives a similar diffraction data [43]. Many of the properties of LDA are those of quasicrystalline material (see [1178]) that would be expected from ES, with its hexagonal and cubic ice substructures. The radial distribution functions of ES show similarities to those of LDA, with both including features similar to cubic [175] and hexagonal ices [41, 1155]. Also, LDA shows crystalline-like behavior in its physical properties (thermal conductivity [617], inelastic incoherent neutron scattering [41] and dielectric relaxation [1155]) with strong similarities to hexagonal and cubic ice [1155]. Neutron diffraction data have been used to suggest the presence of pentamers, boat and chair hexamers and partial dodecahedra [42]. LDA gives an O...O radial distribution function with peaks at 2.79, 4.56, 6.95 and 8.60 Å from X-ray data [43a] whereas the ES gives peaks at 2.80, 4.57, 5.38, 7.06, 7.93, 8.88 and 9.16 Å which reduce to just four peaks at 2.8, 4.6, 6.7 and 9.0 Å, on Gaussian broadening, showing close agreement. The neutron diffraction data [20] gives peaks at 1.8, 2.3, 3.3 (shoulder), 3.8, 4.6, 5.2 (shoulder), 7.7, 8.4 and 9.1 Å and troughs at 2.7 and 6.4 Å. This compares favorably with the calculated distribution function from ES, which gives peaks at 1.8, 2.3, 3.2, 3.8, 4.6, 5.3, 7.3, 8.0 and 9.2 Å and major troughs at 2.8 and 6.8 Å. This material is the same density [34] as ES and may bear some relationship to it, particularly as clusters with icosahedral symmetry cannot form crystals and therefore must form amorphous solids or quasicrystals. The similarities between ES and LDA are reinforced by the deformation and diffusive behavior of LDA as a viscous liquid rather than a solid ice [334]. The phase transitions found by some in supercooled water [44, 45] may be due to the same reasons as the sharp transition between the puckered (CS) and non-puckered (ES) water clusters seen in the molecular mechanics optimizations; the ES structure showing both the perfect tetrahedrality and possessing exactly four nearest neighbors^b as found to be required by modeling [498]. A study of homogeneous nucleation rates in supercooled water has found two rate constants, the slower one of which can be assigned to nucleation of the more strongly hydrogen-bound ES and the faster one to CS nucleation [333]. An ordered arrangement of cavities has been proposed from the diffraction data of LDA [30], also in agreement with the ES model. It has been reported that the entropy of LDA is only a sixth of that than can be explained from a random network model [21] but in good agreement with the much more ordered ES. A Raman spectral study of LDA showed the presence of at least two, or possibly three, distinct species [46] in line with three in the ES model. Raman spectra have also shown the similarity between LDA and glassy tetramethylammonium chloride solution [167], a proposed ES-like structure (see above). Further support for an ordered (for example, ES-like) model for LDA has been given by inelastic neutron scattering [175].

Clathrate-like structures are here proposed as being part of the normal structure of water, albeit in a mainly puckered state at ambient temperatures and increasingly fragmented at higher temperatures. A number of Raman and X-ray diffraction studies have established local convex clathrate-like structures at atmospheric pressure, which become increasingly important as the water is supercooled [195], or under the influence of infrared radiation [730] or sunlight [1173]. [Clathrate hydrate](#) formation overrides hexagonal ice formation in supercooled solutions [1656]. Molecular dynamics simulations agree, showing that clathrate cages have longer lifetimes at lower temperatures [662] and that [sub-clusters of ES](#) are found in supercooled water [729]. The degree of tetrahedral hydrogen bonding also shows an increase on supercooling as the average water cluster grows [658, 1601]. The proportion of water molecules connected by 4- and 3-hydrogen bonds in supercooled water (250 K) has been calculated, using an atoms-in-molecules approach, to be 41% and 29% respectively [1531]. If water at this temperature consisted of a close-packed arrangement of [ES](#) then it would contain about 42% (4-hydrogen bonded water) and 32% (3-hydrogen bonded water) in close agreement.^a Further support for such clustering is that low density water has been shown to exist around aqueous cavities [1080] and that the resistivity of water [increases considerably at low temperatures](#). Shear viscosity and self-diffusion studies have shown the existence of high concentrations of clathrate-like structures in supercooled water [47]. In particular, water was shown to diffuse through many hydrogen-bonded water pentagons, such as occur through the [spines](#) of [ES](#), where all water molecules [linepathways](#) of large cavities, separated by pentagons. The number of water pentagons required to explain water's anomalies ($\sim 0.13/\text{mol}$) is almost exactly equal to the number in [ES](#) ($36/280$; $0.129/\text{mol}$) at the homogeneous nucleation temperature [366].

[Vicinal water](#), extending for tens of nanometers but well within the unstirred 'Nernst' layer near inert solid surfaces, has been found to have properties consistent with partial conversion to [low-density water](#); for example, reduced density (-4%) and raised dielectric, specific heat (+25%), compressibility (+20-100%) and viscosity (+200-1100%) [205]. The thermodynamic rationale for the formation of this (interfacial) vicinal water is that the loss of hydrogen bonds at the surface increases the enthalpy so necessitating the water molecules to compensate by doing pressure-volume work, that is, the network expands to form low-density water with lower entropy (see also [hydrophobic surfaces](#) and for example, [480]).

Other evidence

Flicker noise spectroscopy indicates the presence of $(\text{H}_2\text{O})_{280}$ clusters at low temperatures [773]. Vibrational spectra have shown the presence of both large clusters (about 240 molecules) [18] and cyclic water pentamers [48] in agreement with [CS](#). Puckering of the pentamers was found to increase with temperature [48]. There are a number of facts that support the presence of some very bent weaker hydrogen bonds in the structure of water. These include the high ice-water energy of fusion, which has been suggested as due to the distortional weakening of a proportion of the hydrogen bonds, and the vibrational Raman spectra [35] that indicates a range of weaker hydrogen bonds. Mid-IR pump-probe spectroscopy of HDO in D_2O has confirmed the existence of two distinct molecular species in water with respect to their orientational relaxation times as would be expected in the strongly-hydrogen bonded [ES](#) and weakly-hydrogen bonded [CS](#) clusters [189]. In particular, the difference in energy between these forms can be deduced from both the Raman scattering in the O-H stretching region and the O-H overtone infrared region to be about half the energy of a hydrogen bond [210]. Factor analysis of the infrared spectra of H_2O and D_2O both show two (and only two) fully hydrogen-bonded species in equilibrium, with their relative concentrations changing with respect to temperature; one predominant at low (supercooled) temperatures and the other at high temperatures, with a 50% crossover at about 30°C [1502]. The transition from [CS](#) to [ES](#) is able to explain the high root-mean-square fluctuations of the intermolecular energy in liquid water (7 kJ mol^{-1}) and the fragile-to-strong^a transition in supercooled water at about 225 K [1040] and close to the [second critical point](#). This has been confirmed by a molecular dynamics study suggesting that liquid water consists of both high-density and low-density amorphous-like regions with a transformation between them in supercooled water [172]. It has been proposed that the observed heat of fusion (6.0 kJ mol^{-1}) is due solely to an increase in bond bending going from ice to water [49]. The average root mean square distortion occurring in [CS](#) is 13.7° , which gives a value very close (5.2 kJ mol^{-1}) to this observed heat of fusion, and also agrees with the 16° distortion estimated from the 600 cm^{-1} libration band [47]. Recently, high resolution oxygen K-edge X-ray emission spectra (XES) of liquid water showed two distinct narrow lone-pair derived peaks, assigned, respectively, to tetrahedral and strongly distorted hydrogen-bonded species, as expected from [ES](#) and [CS](#) structures respectively, with no intermediate structures [1557].



The percentage composition of the low density state of water as determined by the variation in density [1354] (red line, also agreeing with viscosity and refractive index data) and IR absorbance data [1738] (blue line). The two lines are quite close considering that they are from different laboratories using very different data. The difference between the two lines may be explained due to the two 'states' of water not being precise structural forms but mixtures of related structures.

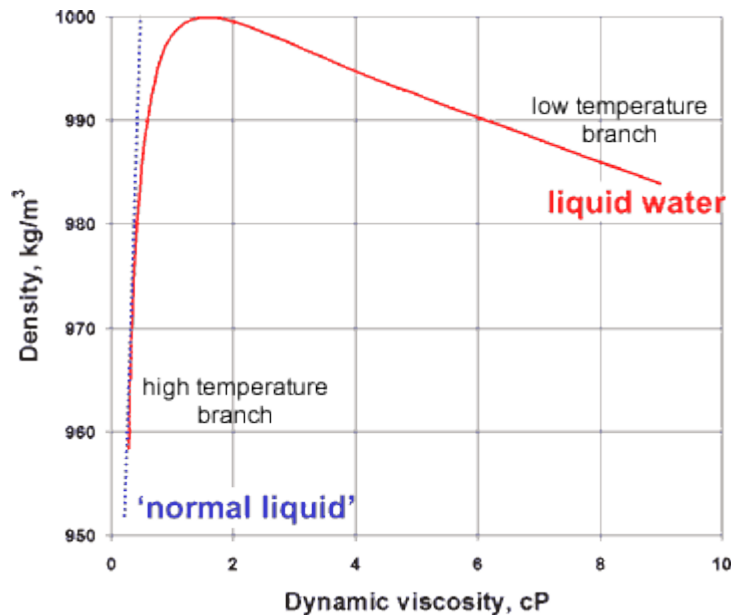
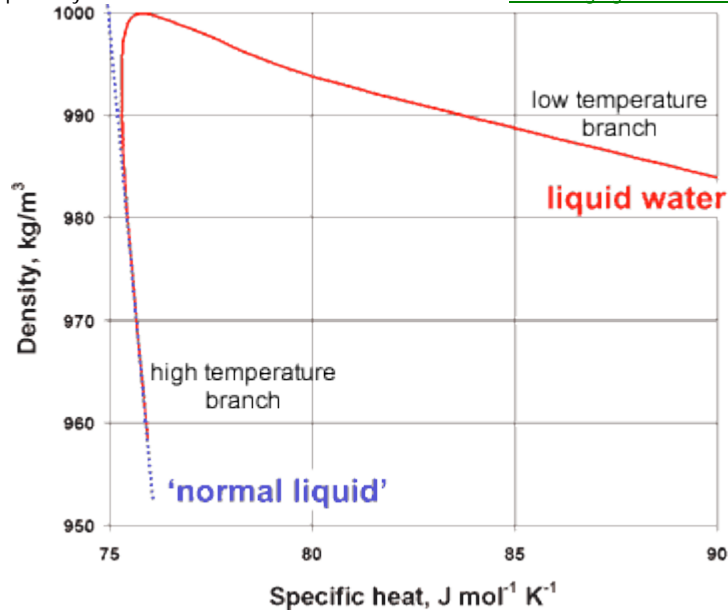
Although still not universally accepted [1520],^f there have been a growing number of papers proposing a [two-state mixture model](#) to explain many of the properties of water

[23, 24, 25, 56, 57, 262, 268, 276, 409, 699, 826, 1150, 1334, 1353, 1354, 1588, 1595, 1603, 1604, 1612, 1639, 1640, 1674, 1738, 175

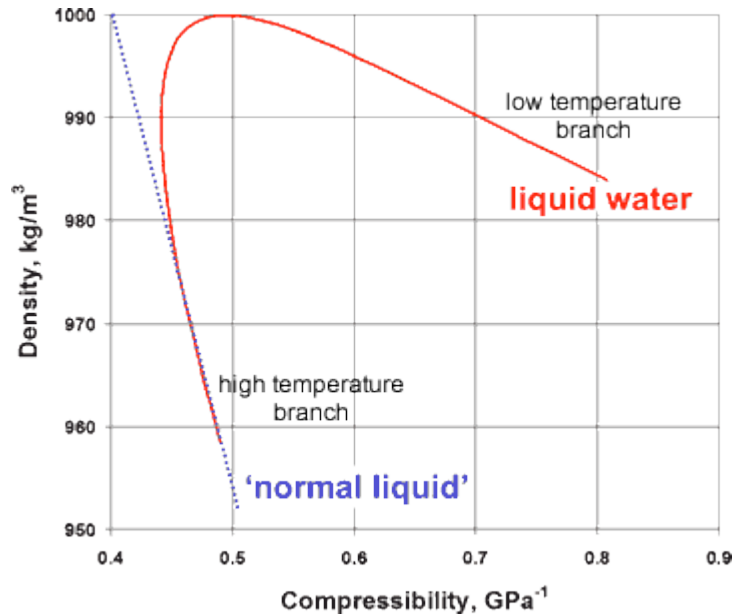
[7, 1763, 1859, 1909, 1980, 1996, 2019, 2051] and has been used to construct an equation of state for supercooled water [2089]. Also, aqueous solutions of 'miscible' solutes may give rise to mesoscopic near-spherical Brownian aggregates of a size from a hundred to a few hundred nm, so showing the presence of separated two-state aqueous systems [1725]. All these proposals are consistent with the ES and CS cluster model.

The great increase in the resistivity (= 1/conductivity) of water at low temperatures [737] indicates the increased formation of localized and limited isotropic hydrogen bonding, so preventing lengthy directed proton movements. The electrical conductivity of water, which increases on degassing [711], also supports this view, as dissolved non-polar gasses promote the formation of ES clusters at low temperatures .

The existence of such equilibrium also enables an explanation of the way some organisms produce low-density water to protect against desiccation [278] and high temperatures [279] and pressures [280]. More ES clusters are found on irradiation with sunlight [1589], probably due to a combination of more structured water absorbing light at about 270 nm[1328] and interactions with the evanescent wave.



The presence of a two phase system can be shown more dramatically from the changes in the compressibility, viscosity and specific heat with the density of liquid water (at constant pressure), where the properties of liquid water can clearly be seen to tend to different behavior at the extremes of the parameters.

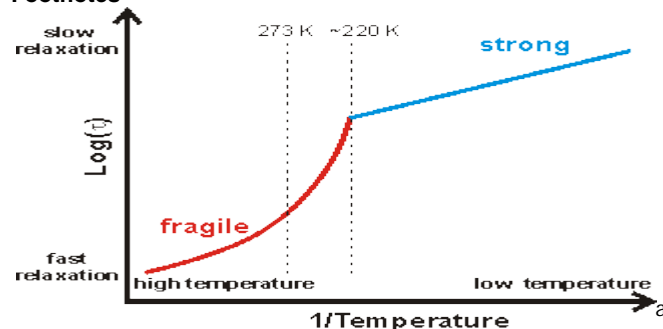


The minimum number of possible arrangements of hydrogen bonds in the fully occupied low-density icosahedral network (ES) is $2^{130} \times 7^{12}$ (curiously this number equals close to 1.50^{280}) as determined during the molecular building. This is in agreement with the minimum entropic factor expected of 1.5 structural variations per molecule [8].

The cluster size (~2.8 nm diameter) is close to that found (~3 nm diameter [140]) to be the limit below which crystalline components in aerosol ice clusters cannot be found and also close to the critical bubble volume found by acoustic cavitation in cold water [1642]. A pronounced peak at slightly greater diameter (~3.4 nm) has been found in aqueous aerosols using a differential mobility particle sizer [141] and a peak at ~3 nm is found in negatively charged waterfall aerosols [2049]. A similarly sized cluster (~2.5 nm) has been found in negatively charged nanodroplets formed from splashed water [1477], where the internal hydrogen bonding is thought to reduce evaporation and prolong the droplet lifetime. A similarly explained cluster (3.4 nm) has been found as an icosahedral aqueous cluster of thirteen fullerene C₆₀ molecules [271]. The same length scale has been found in an interesting experiment [912] where a tiny water pool (~10⁻²³ liter) is stretched between hydrophilic surfaces using an atomic force microscope; the thread of capillary meniscus water having its final "sticking" position at 3.1 nm and breaking when 4.2 nm long and 2.6 nm wide and with "sticking" steps roughly equivalent to the icosahedral water cluster cavity positions. A diameter of about 2 nm has been determined for water clusters in cold water by the use of acoustic phonons [1162].

The proposed structure fits the much-promulgated theory of how sugar molecules interact with water, based on anisotropic hexagonal ice-type interactions [5, 52], but allows sugars a wider range of orientations. Thus, in a solution of scyllo-inositol, each hydroxyl group can both donate and accept a hydrogen bond so long as the scyllo-inositol is situated in one of the 80 chair-form hexagonal sites with different orientations within each 280-molecule cluster. Thus many sugars are able to create locally-stabilized areas within the network of icosahedral clustering. ES may also be formed as a major part of the low-density water reported to form in gels and at the surface of some macromolecules [4] where an orientation effect may be expected to strengthen the hydrogen-bonding in the water.

Footnotes



Fragile liquids, such as liquid, and mildly supercooled, water

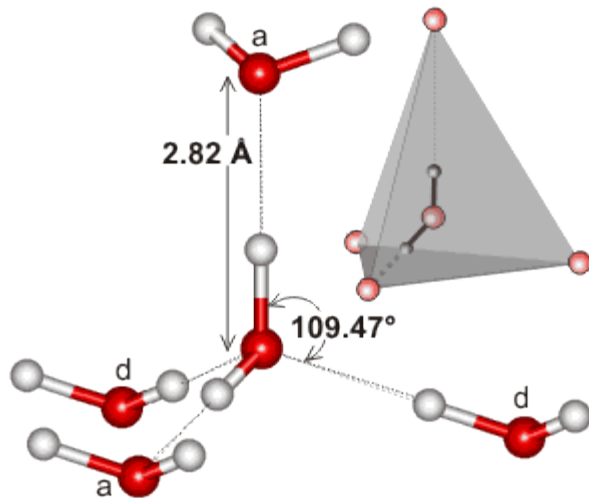
(higher density, more fluid), have a large heat capacity and exhibit non-Arrhenius behavior (that is, log(viscosity) varies non-linearly with the

reciprocal temperature; for example, $\tau_T = \tau_i e^{DT_0/(T-T_0)}$, where τ_T is the structural relaxation time, τ_i is a constant related to the relaxation of liquid water, D is the degree of fragility, T is the temperature and T_0 is the Kauzmann temperature where divergence from Arrhenius behavior (see below) [1078] due to the molecular structuring changing with temperature [1075]. Fragility can be a consequence of clustering producing no long range density ordering. Strong liquids, such as [deeply supercooled water](#) (low density, less fluid), have small heat capacity and exhibit Arrhenius behavior (that is, $\log(\text{viscosity}) \propto 1/\text{temperature}$; $\tau_T = \tau_i e^{E_A/RT}$) where the structuring changes little with temperature [232], and the density fluctuations are minimal.

The apparent fragile-to-strong transition in water (at about 220-225 K [1040, 1078, 1200]) has been explained [558] as being a consequence of the [balance](#) between hydrogen bonding effects (low entropy found in low density water) and the van der Waals dispersion forces (higher entropy) being disturbed in favor of the hydrogen bonding alone at lower temperatures. The [temperature coefficient of the specific heat](#) changes sign with this transition. [Back]

There is a measure for the degree of uniformity (τ) in the H₂O-H₂O hydrogen bond lengths (the translational order parameter, also the degree of order in the local density) in the same way that [tetrahedrality](#) measures H₂O-H₂O-H₂O angle uniformity. The density order

parameter $\tau = \frac{1}{\xi_c} \int_0^{\xi_c} |g(\xi) - 1| d\xi$ where $\xi = r\rho^3$ and r is the O...O distance, ρ is the density, ξ_c is a suitable cut-off distance [1082]. The density order tends to a minimum as the tetrahedrality tends to a maximum. [Back]



Note that the main peaks indicate that the principal feature in liquid water (as in ice) is a water molecule at the center of a tetrahedron of water molecules with O...O ~2.8 Å and ~4.6 Å, O...H ~1.8 Å and ~3.3 Å and H...H ~2.4 Å and ~3.6 Å. There is no difference between the acceptor (a) or donor (d) hydrogen bonding water molecules. Peaks due to O-H (~1.0 Å) and H...H (~1.6 Å) distances within the same molecules are always excluded from such analyses. [Back]

Although this reference [1476] discusses additional clathrate structures, the icosahedral clusters discussed here also contain O...O radial distribution maximum at ~1.06 nm and are supported by the data presented, with maximum ~1.08 nm. [Back]

Calculated on the basis of 74% close-packing and hydrogen bonding numbers as calculated from the [ES](#) structure and shown [on another page](#). [Back]

A two-dimensional Raman-terahertz (THz) spectroscopy study [2050], cited as non-supportive of the [two-state mixture model](#), rules out persistent structures but does not invalidate [cluster formation](#) and supports heterogeneities in water.

Source: <http://www1.lsbu.ac.uk/water/evidnc.html>